

https://doi.org/10.1070/QEL16906

New approach to terahertz diagnostics of human psychoemotional state

E.E. Berlovskaya, O.P. Cherkasova, I.A. Ozheredov, T.V. Adamovich, E.S. Isaychev, S.A. Isaychev, A.M. Makurenkov, A.N. Varaksin, S.B. Gatilov, N.I. Kurenkov, A.M. Chernorizov, A.P. Shkurinov

Abstract. **A new approach to terahertz (THz) diagnostics of the human psychoemotional state is proposed, based on the analysis of the THz contribution to the total signal while simultaneously recording the IR and THz emissions from the human body (hereinafter referred to as the IR–THz image). The developed image-processing algorithm allows extraction of the informative contribution determined by the THz radiation from the total signal perceived by the recording system. Simultaneous registration of the IR–THz images of the human face and the psychophysiological indicators are carried out in situations of physical stress (short-term intense physical exercise – squats functional test), electrical stimulation, and information stress (cognitive load – simple arithmetic mental calculations). The obtained data are compared with those of similar measurements at rest. It is shown that using cluster analysis of IR–THz images it is possible to divide the test subjects into classes according to the type of reaction of the circulatory system under stressful conditions.**

Keywords: *infrared radiation, terahertz radiation, instrumental contactless psychodiagnostics, instrumental methods of research, psychophysiology, psychoemotional states.*

1. Introduction. Formulation of the problem

Objective (psychophysiological) diagnosis of the psychoemotional state (PES) of a person (emotions, stress, anxiety, fears, depression) is an extremely important and socially significant problem that needs to be addressed in various fields of activity, for example, in areas of technology with an increased risk of man-made disasters (atomic stations, transport, chemical industry). Traditional methods for assessing human PES are contact methods that use special sensors superimposed on the surface of the body and convert the activity of the human nervous, muscular and cardiovascular systems into electrical signals of measuring devices [1, 2]. The development of modern diagnostic PES technologies is characterised by the transition from contact methods to remote ones (bio radar, laser Doppler vibrometry, eye tracking, audio and video recording, infrared thermography, etc.) that allow PES to be assessed in real time [1] without contacting the object of study.

The creation of new remote diagnostic methods for PES is closely related to the development of advanced modern technologies. One of the promising areas of development of such methods is the analysis of the relationship between the objective condition of a person and his own electromagnetic radiation in various spectral ranges or features of the reflection of weak radiation from surrounding objects. It is well known that the human body is a source of electromagnetic radiation, whose frequencies occupy a range that begins from a few tenths of a hertz and covers the radio frequency, microwave and IR ranges, as well as the visible part of the spectrum [3].

An image is perceived by man through the organs of vision. The human eye is a fairly inertial optical device and perceives only a relatively small part of the spectrum of electromagnetic radiation emitted or reflected by objects (from 0.38 to 0.75 μm). The quality measure of a biological, electronic, and other technical vision system is the ratio of the amount of information perceived by this system to the amount of information contained in the radiation flux entering the imaging system [4]. In most cases, the image of an object obtained in the region of radiation invisible to the eye is radically different from the images in the visible part of the spectrum. This is usually caused by different conditions of absorption, reflection and radiation by objects in different regions of the spectrum [3]. Almost all physiological and biochemical processes occurring in the human body are accompanied by a change in its own electromagnetic radiation in different frequency ranges. Changes in the state of the body as a result of internal processes or exposure from outside inevitably cause variations in the intensity and nature of its own electromagnetic radiation, including changes in the reflection coefficient of the skin surface, which is an objective diagnostic criterion [3]. Most of the natural radiation from the surface of human skin lies in the IR range and corresponds to wavelengths from 4 to 50 μm, while its maximum falls on waves with $\lambda = 10$ μm.

E.E. Berlovskaya, I.A. Ozheredov, A.M. Makurenkov Faculty of Physics and International Laser Centre, M.V. Lomonosov Moscow State University, Vorob'evy Gory, 119991 Moscow, Russia; e-mail: berlovskaya.elena@mail.ru;
O.P. Cherkasova Institute of Laser Physics, Siberian Branch, Russian Academy of Sciences, prosp. Akad. Lavrent'eva 13/3, 630090 Novosibirsk, Russia; Novosibirsk State Technical University, prosp. Karla Marksa 20, 630092 Novosibirsk, Russia; e-mail: o.p.cherkasova@gmail.com;
T.V. Adamovich, E.S. Isaychev, S.A. Isaychev, A.M. Chernorizov Faculty of Psychology, M.V. Lomonosov Moscow State University, Vorob'evy Gory, 119991 Moscow, Russia;
A.N. Varaksin, S.B. Gatilov, N.I. Kurenkov CJSC Pattern Recognition Research Company, Profsoyuznaya ul. 84/32, stroenie 14, office 603, 117485 Moscow, Russia;
A.P. Shkurinov Faculty of Physics and International Laser Centre, M.V. Lomonosov Moscow State University, Vorob'evy Gory, 119991 Moscow, Russia; Institute on Laser and Information Technologies, Federal Scientific Research Centre 'Crystallography and Photonics', Russian Academy of Sciences, Svyatoozerskaya ul. 1, 140700 Shatura, Moscow region, Russia

Received 26 September 2018; revision received 2 November 2018
Kvantovaya Elektronika **49** (1) 70–77 (2019)
Translated by V.L. Derbov

In the range of 5.6–25 μm, human skin emits infrared waves as a black body, regardless of its individual characteristics, therefore, the emissivity of the skin is considered close to unity [5].

In recent years, results have been obtained on the use of human thermal radiation of the IR range (thermography) for solving various medical problems, for example, in diagnosing pathologies of the spinal cord and brain [6], pathologies of the peripheral nervous system [7], and in inflammatory processes [8].

Changes in local temperature associated with the activity of the facial muscles involved in the expression of emotions can be measured remotely using an IR digital camera. This allows non-contact recording of a set of stereotyped behavioural reactions (patterns) of facial muscle activity and, thus, recognising the emotions associated with these patterns [9]. A number of studies have confirmed a clear correlation between emotions, stress levels, pain and anxiety, on the one hand, and changes in blood flow in the skin area of the face, on the other hand [10–14]. In Ref. [10], data are presented on the possibility of using IR images as a basis for quantifying such parameters of the activity of the autonomic nervous system as local blood perfusion, heart rate (HR) and respiration rate. In Ref. [11], it was shown that the level of perfusion in the orbital region allows one to register small temperature changes associated with human PES. The authors of Ref. [12] have found that for the diagnosis of stress the rectangular area of the forehead containing central vessels is most informative.

The development of the THz imaging technique in recent years has raised the question of whether human radiation in this frequency range provides additional information. It is expected that the registration of the thermal image of the human body using thermal imaging technology, while expanding its spectral sensitivity in the THz frequency range, should lead to the informative contribution determined by new physiological indicators, such as peripheral blood circulation, sweating, etc., and related changes in the refractive index of the skin and its transmittance. This should potentially allow the recording of changes in the psychological state of a person by objectively recording his physiological parameters.

The purpose of this work is to develop a new approach to the THz diagnosis of human PES, based on the analysis of the THz contribution to the total signal while simultaneously recording the IR and THz emissions of a person's face.

The spectral density of the luminosity of the human body (excluding evaporation, heat exchange, clothing absorption, etc.) [15], as well as the spectral sensitivity of the widely used FLIR thermal imaging camera [16] and the multichannel IR–THz detector NEC [17], whose analogue is used in this work, are schematically presented in Fig. 1. The spectral sensitivity range of the FLIR infrared detector with the SC7790VL matrix based on mercury cadmium telluride corresponds to the maximum of the luminosity spectrum of the human body. However, a significant part of the infrared radiation energy, corresponding to the long-wavelength wing of its spectral distribution, does not fall into the sensitivity region of a thermal imaging camera, which imposes significant restrictions on the diagnostic informativity of IR thermal imaging methods. These limitations can be removed using infrared detectors with a sensitivity range expanded in the THz region, for example, the NEC IR/V-T0831C detector based on an array of microbolometers, the spectral range of which is shown in Fig. 1.

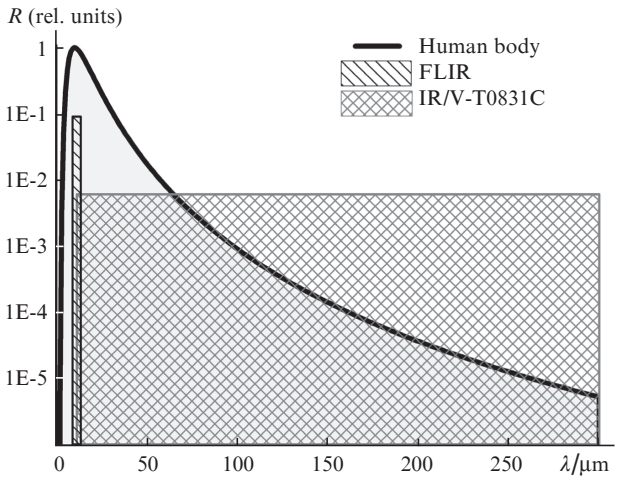

Figure 1. Luminosity spectrum of the human body [15] and the spectral sensitivity ranges of the FLIR SC7790VL [16] and NEC IR/V-T0831C [17] detectors.

Figure 2. Instrumental diagnostic complex for contactless scanning of the face skin: (*1*) IR/V-T0831C detector; (*2*) monitor with a programme of psychoemotional stimuli; (*3*) chair with backrest tilting drive.

2. Instrumental diagnostic complex. Measurement procedure for IR–THz images

Registration of IR–THz images and psychophysiological parameters of the subjects was carried out using an instrumental diagnostic complex, including the IR–THz detector

NEC IR/V-T0831C, the software package 'Egoskop' (version 3.3.2, developed by Medicom MTD) [18], the personal computer and the seat with backrest drive (Fig. 2). The IR/V-T0831C detector allows the registration of IR–THz images of the object under study in the spectral range from 1 to 30 THz (from 9 to 300 μm).

In the process of recording and analysing IR–THz images, it was revealed that involuntary head movements associated with the stabilisation of the body in space have a noticeable effect on the results of image processing, and this must be taken into account when further developing sensors for diagnosing PES in real time. In order to minimise the detected phenomenon, all subjects were located in a chair in a reclining position, as shown in Fig. 2.

3. Classification of subjects

In preliminary experiments, a complex program was developed and tested for synchronous recording of own electromagnetic radiation from the person tested in the THz frequency range and a number of psychophysiological indicators in the simulation of stress situations differing in the nature and intensity of the impact [19]. For inducing stress effects, we used a physiological stressor in the form of electrical stimulation, an information stressor in the form of cognitive load (math problems on the multiplication of two-digit numbers), and a physical stressor in the form of short-term intense physical exercises (squats). During the experiment, contact methods were used to record indicators of the activity of the central nervous system [electroencephalogram (EEG)] and the peripheral nervous system [electrocardiogram (ECG), heart rate (HR), photoplethysmogram (systolic wave amplitude, SWA), galvanic skin response (GSR)]. The average values of indicators were analysed at each stage of testing. A group of 38 volunteers took part in the experiments (20 men and 18 women). The age variation of the subjects was from 19 to 57 years (the median was 24 years, the absolute deviation of the median was 3 years).

The results of preliminary experiments showed that there is a qualitative and quantitative specificity of psychophysiological patterns depending on the nature and intensity of the stress effect. Using the Wilcoxon test for paired samples, we found that, in comparison with the initial background, the response to pain during electrical stimulation causes a slight narrowing of blood vessels and high GSR activity. The response to cognitive load is accompanied by a less pronounced activity of GSR, but a greater vasoconstriction, as well as an increase in the rhythm of heart contractions and a decrease in the ratio of EEG alpha and beta rhythms [19]. Significant differences in the manifestation of the psychophysiological reaction to stressful effects depending on gender, age and body weight of the subjects could not be found.

4. Results and discussion. Informative image processing algorithm

In the process of analysing the IR–THz images of the subjects' faces, image histograms were constructed. The maximum value of the histogram varies noticeably from frame to frame. In addition, the histogram method of analysing IR–THz images showed that a small part of the histogram (no more than 2%), which carries information about the structure of the useful signal, is of interest. The problem that arises is how to extract useful information corresponding to a small portion of the histogram fluctuating in a known range.

To obtain a pseudo-colour image, a histogram is constructed, all points of which are divided into three clusters (Fig. 3) by using two adaptive thresholds P1 and P2, varying from frame to frame, while maintaining a symmetrical arrangement relative to the maximum of the histogram.

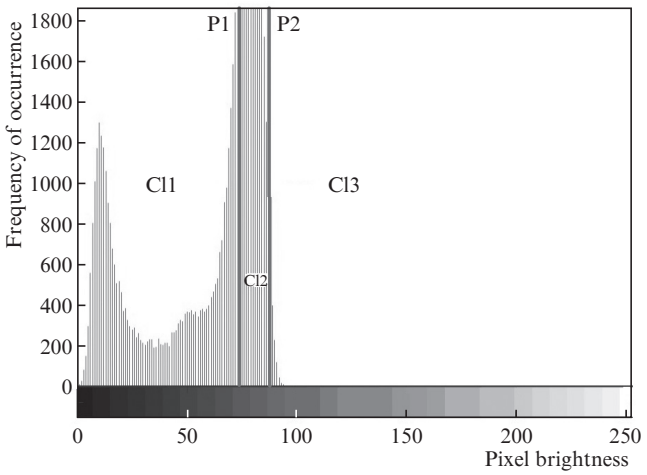

Figure 3. Histogram with two adaptive thresholds P1 and P2, forming three clusters (Cl1, Cl2, and Cl3).

Figure 4 shows the original IR–THz image (left) and pseudo-colour image (right), resulting from the clustering of pixel brightness values into three classes. Based on the studies performed, the IR–THz images significant for the diagnosis of PES, highlighted in Fig. 4 (right) in green, are the following: the frontal part, the eye area shifted to the nose; muscle area, raising the angle of the mouth; lips and parts of the neck. It should be mentioned that in the analysis of infrared images of a human face, there are areas in which the temperature noticeably rises under stress, such as a rectangular forehead area [12] and the orbital area [11], as well as the tip of the nose, where there is a decrease in temperature during exposure [20, 21].

The histogram Q for brightness images X consists of n cells with the interval width $A/(n-1)$, q being the frequency

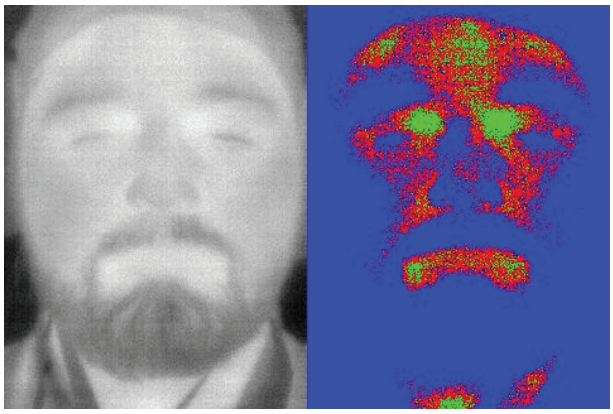

Figure 4. (Colour online) Original IR–THz image in black and white (left) and pseudo-colour image (right).

of occurrence of elements in the image. The belonging x of the image element to the brightness interval $Q(d)$ is determined from the condition

$$\frac{A(d-1.5)}{n-1} \leqslant X < \frac{A(d-0.5)}{n-1}, \quad (1)$$

where A is a scale factor depending on the type of image (in our case, the image is a 8-bit one, for such images $A = 255$); n is the number of intervals; and d is the sequence number of the current interval.

Background points that do not belong to the face form the first cluster (Cl1) and points of the object that belong to the face form the second cluster (Cl2). Characteristic points of increased intensity belonging to the face form the third cluster (Cl3) (see Fig. 3). Note that the cluster division is implemented using the threshold method with the threshold values P1 and P2 calculated automatically according to the results of the analysis of the histogram of each IR–THz image, taking into account the change in the parameters of the maximum expressed as

$$[s, b] = \max(Q), \quad (2)$$

where b is the maximum value; and s is the sequence number on which the maximum value is reached.

This allows automatic adaptation of thresholds from frame to frame. The thresholds P1 and P2, forming the second cluster, are set symmetrically to the left and to the right relative to the maximum of the histogram of the entire image, the value of which varies from frame to frame. The values of the thresholds P1 and P2 are calculated using the expressions

$$\mathrm{P1} = b - (A - b)/k, \quad (3)$$

$$\mathrm{P2} = b + (A - b)/k, \quad (4)$$

where k =2, 3 is a coefficient depending on recording conditions.

Thus, the image points that satisfy the condition

$$0 \leqslant x < \mathrm{P1}, \quad (5)$$

belong to the first cluster. Image points corresponding to the interval

$$\mathrm{P1} \leqslant x < \mathrm{P2}, \quad (6)$$

belong to the second cluster. Finally, the image points corresponding to the interval

$$\mathrm{P2} \leqslant x < 256, \quad (7)$$

belong to the third cluster.

Statistical analysis of the quantitative composition of the three clusters defined above for the series of IR–THz images has shown that in the first and second cluster the number of points varies from frame to frame in antiphase. In other words, an increase in the number of background points leads to a decrease in the number of 'warm' points of the face, and vice versa (Fig. 5). This circumstance is associated with the accumulation time control algorithm and the gain of the IR–THz detector, whose operation is consistent with the principles of fuzzy logic. As a result, the intensity of the image harmonically precesses in the neighbourhood of the quasi-optimal solution. At the same time, the change in the quantitative characteristics of the third cluster from frame to frame has no pronounced correlation with the quantitative composition of the other two clusters and is directly related to the formation of the useful signal. We believe that the change in the number of points in cluster 3 depends on the processes of blood vessel filling caused by the contraction of the heart

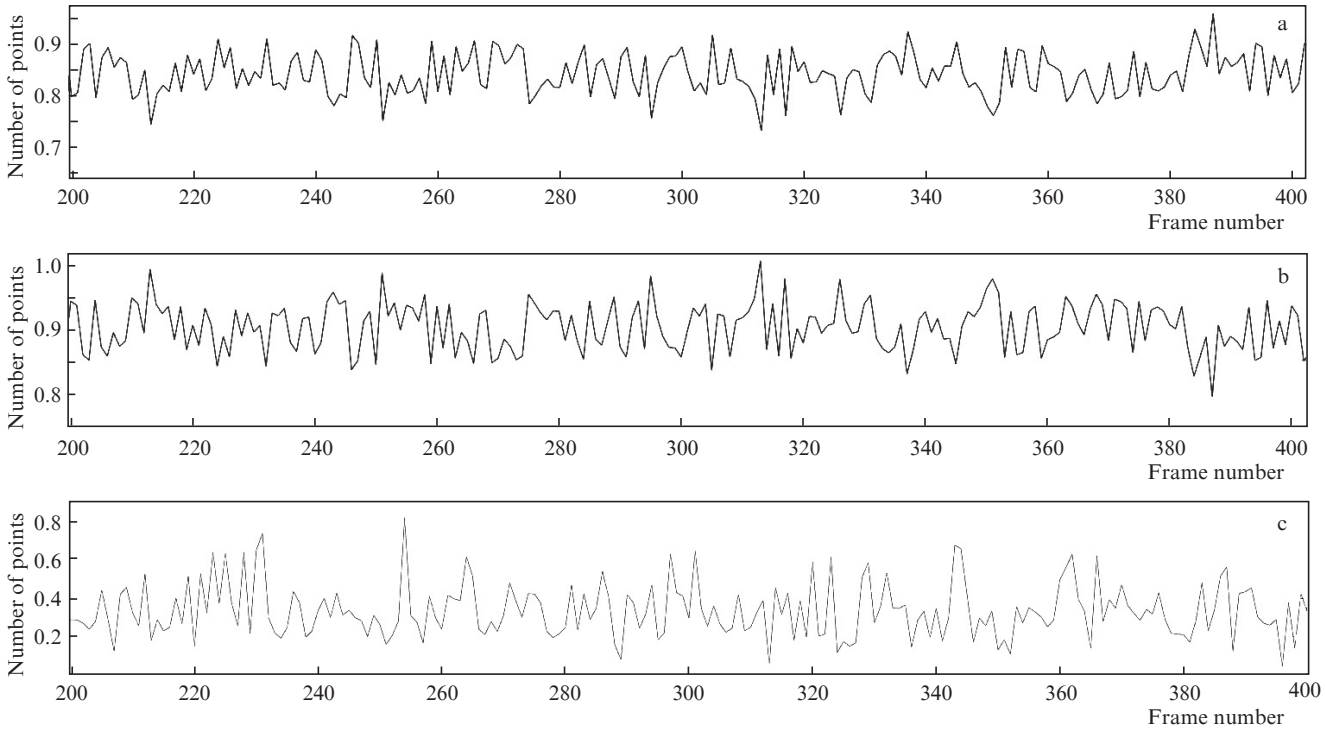

Figure 5. Varying number of points in clusters (a) 1, (b) 2 and (c) 3 vs. frame number.

muscle. Extrema of the received signal (Fig. 5c) correlate with the heart rate. The formation of the useful signal occurs at a frequency of 8 Hz (associated with the appearance of a frame on the time axis), and the signal is formed as a superposition of several distributed signals recorded from different parts of the face. Despite the fact that the excitation function is heart rate, the response we register is rather complex and requires the refinement of various physical models, primarily hydrodynamic, associated with the filling of vessels with blood.

The distribution diagrams of the corresponding values shown in Fig. 6 characterise the visualisation of the number of points of the second and third clusters normalised to a unit, obtained in the course of the mathematical data processing. The abscissa is the normalised value of the number of points of the second cluster, and the ordinate is the corresponding num-

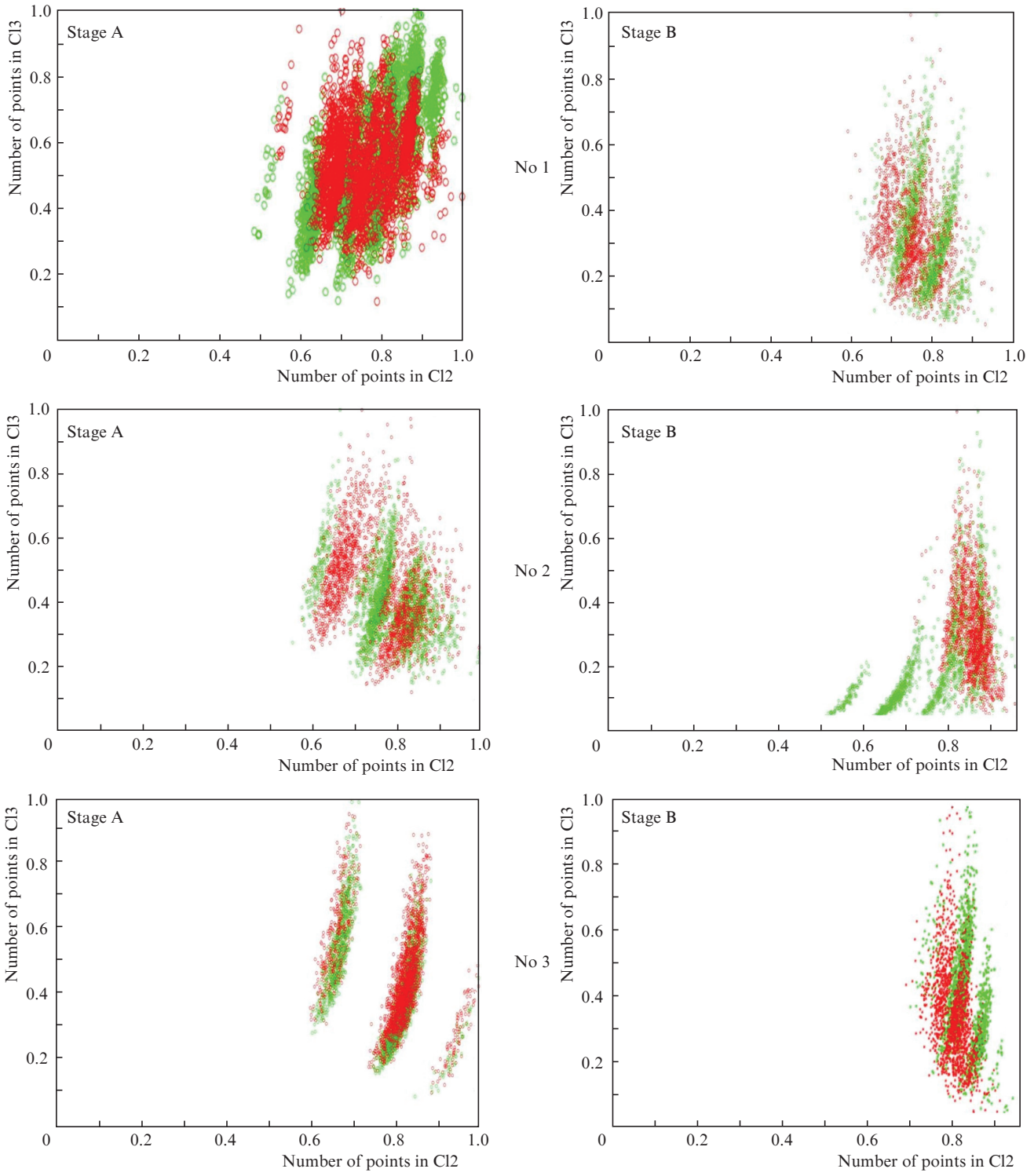

Figure 6. (Colour online) Distribution diagrams of the second and third clusters normalised to a unit for subjects (No. 1 – No. 3) at the first (A) and repeated (B, after 20 days) testing stages. Green dots indicate calm state, and red dots – stressful state.

Table 1.

Subject number	Sex	Age	HR (1st series)/bpm		HR (2nd series)/bpm	
			Baseline	After exposure	Baseline	After exposure
1	female	21	84 ± 3	87 ± 3	78 ± 4	86 ± 5
2	female	21	74 ± 5	70 ± 6	93 ± 3	81 ± 6
3	male	21	68 ± 8	72 ± 9	76 ± 4	98 ± 14

ber of points of the third cluster. The results of processing the images of the subjects after testing with an interval of 20 days are shown. The characteristics of the subjects and the value of the heart rate, measured by the standard contact method, in the initial state and after exposure are presented in Table 1.

As seen from Fig. 6, some bands can be distinguished in the diagram, which differ in the number of points of the second and third clusters. One can assume that their number and structure are associated with the blood filling of the vessels of the human face. As shown in Section 3, the stimuli we use lead to changes in the lumen of the blood vessels and heart rate. Overlaying scatterplots for stress and calm states on one graph allows one to notice the shift of scatterplots to the left or to the right when exposed. The use of diagrams allowed the tested persons to be classified according to changes in the blood supply under stress. Thus, in some people stress causes a rush of blood (see Fig. 6; No. 1 and No. 3) and an increase in heart rate (see Table 1). In this case, there is some shift of the diagrams to the left relative to the initial state. In other subjects, stress causes a decrease in heart rate, vasospasm and a decrease in the intensity of blood circulation (Fig. 6; No. 2). In this case, there is a shift of the diagram to the right.

In a series of experiments conducted at different times on the same subjects (with an interval of 20 days), the repeatability of the reaction to a stressful effect is demonstrated: the scatter diagrams in the subjects are shifted in the same direction as in the first experiment (see Fig. 6). The dynamics of changes in heart rate after stress exposure is also repeated (see Table 1). This demonstrates the repeatability of the reaction to the reproduction of a stressful situation. This means that the displacement of scatter diagrams in a stressful situation is determined by the individual psychophysiological characteristics of the subjects.

Figure 7 presents IR–THz images showing the dynamics of changes in the intensity of significant points (green) with increasing stress load.

It is known that the vegetative nervous system [22] regulates the blood supply to the peripheral blood vessels of the

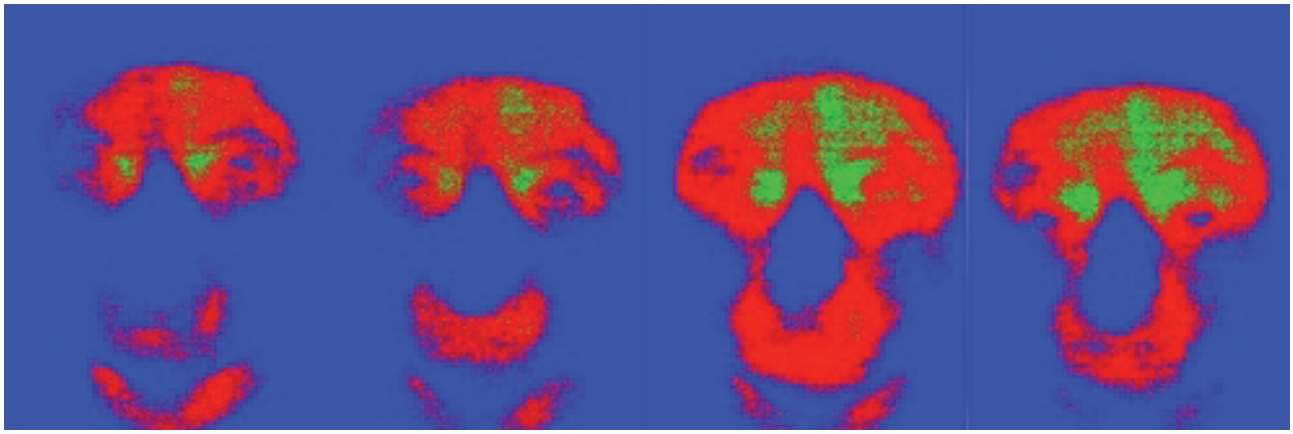

Figure 7. (Colour online) Dynamics of change (from left to right) of the number of significant points (green) in the IR–THz image of a human face as the stress load increases.

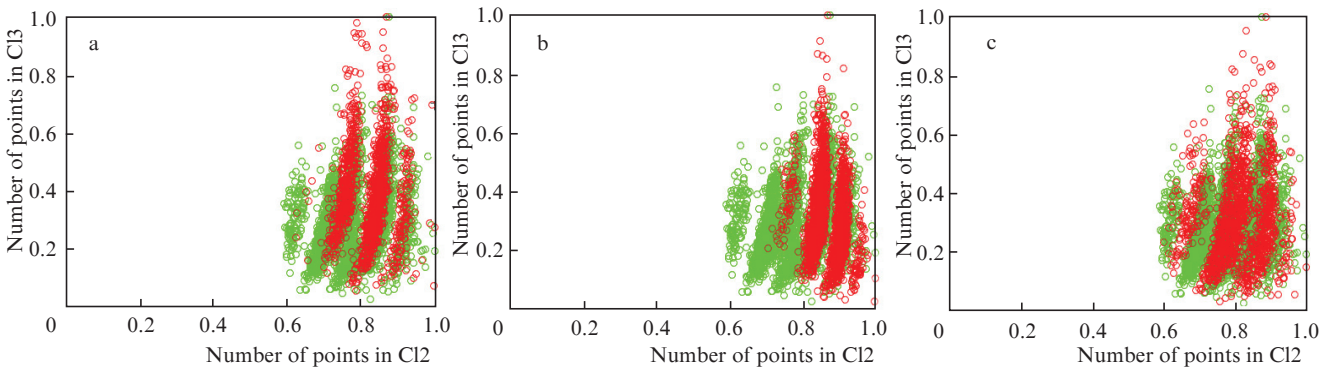

Figure 8. (Colour online) Distribution diagrams of the second and third cluster points normalised to a unit for sympathotonic persons before and after stress exposure: (a) cognitive load; (b) electrostimulation; and (c) functional test (squats).

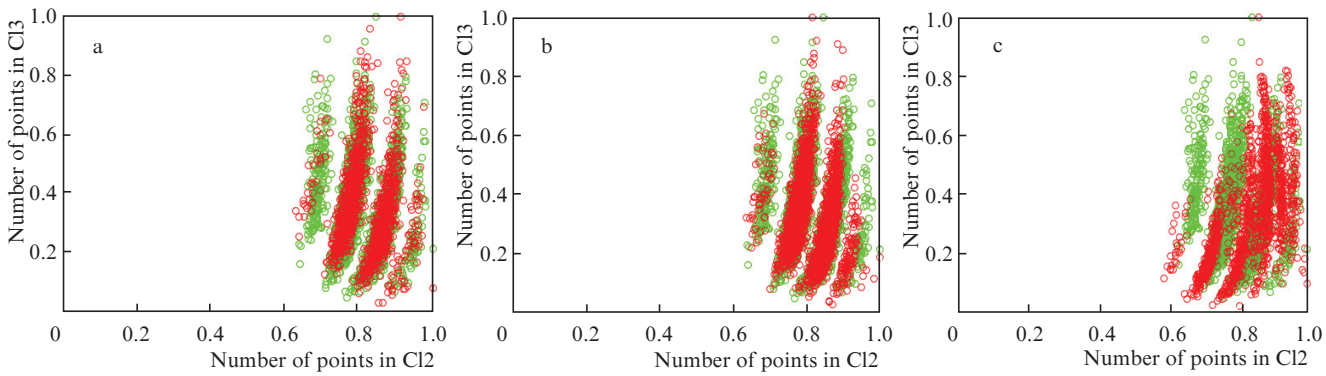

Figure 9. (Colour online) Distribution diagrams of the second and third cluster points normalised to a unit for normotonic persons before and after stress exposure: (a) cognitive load; (b) electrostimulation; and (c) functional test (squats).

skin. The response to stressful effects depends on the balance of the constituent parts of this system, namely, its sympathetic and parasympathetic components [23]. Figure 8 shows diagrams of the distribution of the second and third cluster points normalised to a unit for persons characterised at rest by a pronounced shift of the vegetative balance towards the sympathetic nervous system. The subjects from this group show pronounced reactions in situations of informational stress, electrical stimulation and physical stress. In this case, there is a shift of the diagram to the right.

Similar diagrams for persons characterised by a balance of sympathetic and parasympathetic nervous systems (normotonic persons) are presented in Fig. 9. For subjects from this group, no shift of the diagram in the dynamics of stress exposure is observed.

When analysing the sequence of IR–THz images, a periodic change in the number of background points in the nose area was also detected. As the inhaled air flow cools the tissues of the nose, the number of background points increases. Then, due to the blood flow, the nasal tissues are heated to the initial temperature, which leads to a decrease in the number of background points. The revealed regularity makes it possible to fix respiratory cycles by analysing IR–THz images.

5. Conclusions

A new approach to the THz diagnostics of human PES based on the analysis of the THz contribution to the total signal of simultaneously registered human infrared and THz emissions is proposed and tested for the first time. Using the developed image processing algorithm, we extract from the full signal perceived by the recording system an informative contribution determined by THz radiation in order to demonstrate the possibility of informative diagnostics of PES based on the analysis of the person's own radiation in the IR and THz ranges of the electromagnetic spectrum. The intrinsic radiation of the face skin, detected by the IR–THz detector at room temperature, allows real-time recording of images that can be processed using the proposed mathematical algorithm to obtain objective information about human PES. The proposed image processing technique allows non-contact information, including information about the physiological characteristics of the subject, e.g., heart rate and respiration. It was shown that using the cluster analysis of IR–THz images, the tested persons can be classified according to the type of reaction of the circulatory system under stressful conditions, namely, in some people stress enhances the blood flow, while in others it causes vasospasm and, as a result, a decrease in blood circulation intensity.

It is shown that when a test person inhales, the intensity of the THz contribution to the total IR–THz signal of the radiation from the regions of the wings of the nose decreases. This phenomenon can be used to develop algorithms for contactless registration of the respiratory rhythm based on the analysis of THz images.

Evaluation of PES significantly depends on the nature and condition of the vegetovascular system. We have proposed a mechanism for its remote stratification for estimating vessel filling in time.

The results of the studies show that, despite the relatively low signal-to-noise ratio and low frequency of image recording, it was possible to extract informative THz frequency components of the broadband IR–THz signal and associate them with psychophysiological reactions, confirmed by other methods of objective control. It is obvious that the improvement of IR–THz detectors and the development of new processing methods will allow wide use of the THz range for remote assessment of human PES.

Acknowledgements. The work was partially supported by the Russian Foundation for Basic Research (Grant No. 17-29-02487) and performed using the equipment purchased at the expense of the Development Programme of the Lomonosov Moscow State University until 2020.

References

1. Chernorizov A.M., Isaychev S.A., Galatenko V.V., in *Etnokulturnaya identichnost kak factor sotsialnoy stabilnosti v sovremennoy Rossii* (Ethnocultural Identity as a Factor of Social Stability in Modern Russia) (Moscow: MSU Publ., 2016) Vol. 2, p. 5.
2. Chernorizov A.M., Isaychev S.A., Zinchenko Yu.P., Znamenskaya I.A., Zakharov P.N., Khakhalin A.V., Gradoboeva O.N., Galatenko V.V. *Psychology in Russia: State of the Art*, **9** (4), 23 (2016).
3. Kudryashov Yu.B., Perov Yu.F., Rubin A.B. *Radiatsionnaya biofizika: radiochastotnye i mikrovolnovye elektromagnitnye izlucheniya* (Radiation Biophysics: Radio Frequency and Microwave Electromagnetic Radiations) (Moscow: Fizmatlit, 2008).
4. Rose A. *Vision: Human and Electronic* (New York–London: Plenum Press, 1973; Moscow: Mir, 1977).
5. Lebedenko Yu.I. *Biometricheskiye sistemy bezopasnosti: uchebnoye posobiye* (Biometric Security Systems: A Training Manual) (Moscow: Direkt Media, 2012).
6. Melnikova V.P., Nikiforov E.M., Voronov V.G. *Zh. Nevropatolog. Psikhiatrii im. S.S. Korsakova*, **5**, 555 (1979).

7. Shuvaev V.E. *Perifericheskaya Nervnaya Sistema*, **10**, 129 (1987).
8. Zayats G.A., Koval V.T. *Zdorov'e. Meditsinskaya Ekologiya. Nauka*, **3** (43), 27 (2010).
9. http://compeng.hud.ac.uk/external/research/index.p.
10. Cardone D., Pinti P., Merla A. *Computational and Mathematical Methods in Medicine*, Article ID 984353 (2015).
11. Pavlidis I., Levine J. *Proc. 23rd Annual EMBS Int. Conf.* (Istanbul, Turkey, 2001) Vol. 3, p. 2826.
12. Puri C., Olson L., Pavlidis I., Starren J. *Proc. Conf. Human Factors in Computing Systems* (Portland, OR, USA, 2005) p. 1725.
13. Vianna D., Carrive P. *European J. Neuroscience*, **21**, 2505 (2005).
14. Nakayama K., Goto S., Kuraoka K., Nakamura K. *J. Physiology and Behavior*, **84**, 783 (2005).
15. Bowling Barnes R.B. *Science*, **140**, 870 (1963).
16. https://www.flir.eu/support/products/sc7900vl#Specifications.
17. http://www.nec.com/en/global/prod/terahertz/pdf/NECTHz0831C.pdf.
18. http://www.medcom.ru/medicom/ego.htm.
19. Manaenkov A.E., Adamovich T.V. *Materialy Mezhdunar. molodezhnogo nauch. foruma "LOMONOSOV-2018"* (Proc. of the International Youth Scientific Forum "LOMONOSOV-2018") (Moscow: MAKS Press, 2018).
20. Znamenskaya I.A., Koroteeva E.Yu., Shishakov V.V., Khakhalin A.V., Kuzmicheva E.A., Isaychev S.A., Chernorizov A.M. *Nauchnaya Vizualizatsiya*, **9** (4), 41 (2017).
21. Kosonogov V., De Zorzi L., Honoré J., Martínez-Velázquez E.S., Nandrino J.L., Martinez-Selva J.M., Sequeira H. *PLoS One*, **12** (9), e0183592 (2017); doi: 10.1371/journal.pone.0183592.
22. Ioannou S., Gallese V., Merla A. *Psychophysiology*, **51**(10), 951 (2014).
23. Zhukov D.A. *Biologiya povedeniya: gumoral'nye mekhanizmy* (Behavioural Biology: Humoral Mechanisms) (Saint-Petersburg: Rech, 2007).